4-2017

Large-Scale Deposition of Weathered Oil in the Gulf of Mexico Following a Deep-Water Oil Spill

Isabel Romero
University of South Florida, isabelromero@usf.edu

Gerardo Toro-Farmer
University of South Florida, torofarmer@usf.edu

Arne R. Diercks
University of Southern Mississippi

Patrick Schwing
University of South Florida, pschwing@usf.edu

Frank E. Muller-Karger
University of South Florida, carib@usf.edu

See next page for additional authors

Environmental Pollution 228 (2017) 179–189

Contents lists available at ScienceDirect

Environmental Pollution

journal homepage: www.elsevier.com/locate/envpol

Large-scale deposition of weathered oil in the Gulf of Mexico following a deep-water oil spill☆

Isabel C. Romero [a, *], Gerardo Toro-Farmer [a], Arne-R. Diercks [b], Patrick Schwing [a], Frank Muller-Karger [a], Steven Murawski [a], David J. Hollander [a]

[a] University of South Florida, College of Marine Science, St. Petersburg, FL 33701, USA
[b] University of Southern Mississippi, Abbeville, MS 38601, USA

ARTICLE INFO

Article history:
Received 29 December 2016
Received in revised form
17 April 2017
Accepted 6 May 2017
Available online 20 May 2017

Keywords:
Oil spill
Deepwater Horizon
Hydrocarbons
Sediments
Spatial analysis

ABSTRACT

The blowout of the Deepwater Horizon (DWH) drilling rig in 2010 released an unprecedented amount of oil at depth (1,500 m) into the Gulf of Mexico (GoM). Sedimentary geochemical data from an extensive area (~194,000 km^2) was used to characterize the amount, chemical signature, distribution, and extent of the DWH oil deposited on the seafloor in 2010–2011 from coastal to deep-sea areas in the GoM. The analysis of numerous hydrocarbon compounds (N = 158) and sediment cores (N = 2,613) suggests that, $1.9 \pm 0.9 \times 10^4$ metric tons of hydrocarbons (>C9 saturated and aromatic fractions) were deposited in 56% of the studied area, containing 21± 10% (up to 47%) of the total amount of oil discharged and not recovered from the DWH spill. Examination of the spatial trends and chemical diagnostic ratios indicate large deposition of weathered DWH oil in coastal and deep-sea areas and negligible deposition on the continental shelf (behaving as a transition zone in the northern GoM). The large-scale analysis of deposited hydrocarbons following the DWH spill helps understanding the possible long-term fate of the released oil in 2010, including sedimentary transformation processes, redistribution of deposited hydrocarbons, and persistence in the environment as recycled petrocarbon.

1. Introduction

In 2010 an unprecedented amount of oil (~4.0 millions barrels; U.S. District Court, 2015) was released at 1,500 m depth into the Gulf of Mexico (GoM) after the blowout of the Deepwater Horizon (DWH) drilling rig. The final budget of the oil spilled in 2010 indicates that the intensive efforts to recover the discharged oil reduced the oil in the marine environment (~20% of the leaked mass; McNutt et al., 2012b; Ryerson et al., 2012) to ~3.2 million barrels (U.S. District Court, 2015). Of the total amount of oil that remained in the environment, natural processes like evaporation reduced even more this amount by 5% (Ryerson et al., 2012). About 6% of the leaked mass was burned (Ryerson et al., 2012), and burned residues remained floating on surface waters until deposition on the seafloor (Adhikari et al., 2016; Romero et al., 2015; Stout and Payne, 2016a). Approximately, 10% of the leaked mass formed surface slicks that were transported horizontally or vertically via the formation and sinking of a large marine snow event (Brooks et al., 2015; Daly et al., 2016; Romero et al., 2015). Also, about 36% of the leaked oil formed deep plumes of dissolved and dispersed hydrocarbons (McNutt et al., 2012b; Ryerson et al., 2012) that were dispersed and transported mostly in southwest direction from that DWH site, and evidences indicate some deposition on the seafloor occurred by direct impingement on the continental slope and sinking of oiled marine snow formed at depth (Daly et al., 2016; Romero et al., 2015). The oil budget as well indicates that 23% of the leaked oil mass was unaccounted for due to the difficulty on measuring the amount of oil in coastal and deep-sea sediments (McNutt et al., 2012b), where it could have significant effects on fauna (Montagna et al., 2013; Murawski et al., 2016, (Murawski et al., 2014); Schwing et al., 2015; Tarnecki and Patterson, 2015; White et al., 2012). Previous studies have characterized and quantify this deposition in scattered areas (Allan et al., 2012; Chanton et al., 2015; Harding et al., 2016; Nixon et al., 2016; Romero et al., 2015; Stout et al., 2016a; Valentine et al., 2014), lacking a large-scale integration over multiple environments in the GoM to better characterize the distribution and amount of DWH oil-derived

☆ This paper has been recommended for acceptance by Maria Cristina Fossi.

* Corresponding author. University of South Florida, College of Marine Science, 140 7th Ave. South, St. Petersburg, FL 33701, USA.
E-mail address: isabelromero@mail.usf.edu (I.C. Romero).

http://dx.doi.org/10.1016/j.envpol.2017.05.019

hydrocarbons deposited on the seafloor. Due to the magnitude of the DWH spill and its spatial extent in the GoM, large areal coverage is necessary in order to attempt calculating the DWH oil fraction that reached the seafloor at a regional scale, essential for a broad environmental assessment of impacts from the DWH spill and for future mitigation plans.

The overall goal of this study was to characterize and estimate the large-scale deposition of oil-derived hydrocarbons following the DWH spill using sedimentary geochemical data analyzed by the University of South Florida, the U.S. Government and the British Petroleum (BP), collected within a year after the DWH blowout over an extensive area (~194,000 km^2). We analyzed a wide range of compounds (Aliphatics: C10–C40 *n*-alkanes, isoprenoids, branched alkanes; PAHs: 2–6 ring polycyclic aromatic hydrocarbons and their homologues; biomarkers: hopanoids, steranes, triaromatic steroids) in order to cover major hydrocarbon mixtures that were partitioned within the water column (subsurface plumes and oil slick) due to the released of oil at depth (1,500 m) (Ryerson et al., 2012) and that were transported to different environments in the GoM (Chanton et al., 2015; MacDonald et al., 2015; Murawski et al., 2016; Nixon et al., 2016). Also, due to the natural heterogeneity in hydrocarbon concentrations observed throughout the GoM (Chanton et al., 2015; Nixon et al., 2016; Stout et al., 2016a), hydrocarbon concentrations were compared within sediment core layers to distinct in each site, background to post-spill levels. We used these data to generate a large-scale spatial model of the deposition of oil-derived hydrocarbons post-spill. The results generated define the amount, chemical signature, distribution, and extent of the DWH oil-derived hydrocarbons deposited on the seafloor in 2010–2011 from costal to deep-sea areas in the GoM.

2. Materials and methods

2.1. Temporal patterns of chemical signatures

2.1.1. Hydrocarbon data

Sediments cores from coastal (including bays and estuaries to 15 km out of the coastline), continental shelf (extending from 15 km out of the coastline to the 200 m water-column depth), and deep-sea (from 200 to 2,600 m water-column depth) areas were studied from the collection efforts in 2010–2011 by the University of South Florida (https://data.gulfresearchinitiative.org/data/R1.x135.119:0004/), the U.S. Government (ERMA Deepwater Gulf Response, https://gomex.erma.noaa.gov/, downloaded on June 2013) and the BP (Gulf Science data, http://gulfsciencedata.bp.com/, downloaded on March 2013) (Supplementary Table 1, Supplementary Fig. 1). Only samples with full analysis of >C9 hydrocarbons were used, that includes: Aliphatics (C10–C40 *n*-alkanes, isoprenoids, branched alkanes), PAHs (2–6 ring polycyclic aromatic hydrocarbons including alkylated homologues), biogenic PAHs (Retene, Perylene), and biomarkers like hopanoids (C23–C35), steranes (C27–C29), triaromatic steroids (C26–C28) (Supplementary Table 2). ∑Hydrocarbons was calculated as the sum of all > C9 hydrocarbons studied (excluding biogenic PAHs). The different databases used similar chemical protocols for the analysis of the composition and concentration of hydrocarbons in sediment samples (8015C, 2007; 8270D, 2007; Wang et al., 2006). To assured reliable results, a strict chain of custody, calibration check samples, method blanks, and matrix spike samples were conducted. A more detailed explanation of QA/QC protocol and sample collection can be found in the Analytical Quality Assurance Plan report for Mississippi Canyon 252 (NRDA, 2011) and Stout et al. (2016b).

2.1.2. Background hydrocarbon concentration

Temporal changes in the sediment cores (N = 802) were calculated by comparing the concentration of >C9 hydrocarbons in the surface layer of recently deposited sediments (post-spill layer: 0–2 cm for the coastal and continental shelf area, and 0–1 cm for the deep-sea area) to concentrations in downcore layers of deposited sediment in the previous years (pre-spill layer: 4–10 cm for the coastal area, 2–4 cm for the continental shelf area, and 1–3 cm for the deep-sea area). The boundaries of these layers were set by previous studies using different analytical techniques and demonstrating that the sedimentary surface layer is composed of a large and rapid deposition of sediments including organic rich compounds (e.g. hydrocarbons) from the DWH spill in 2010 (Brooks et al., 2015; Chanton et al., 2012; DWH Trustees, 2015; Lin and Mendelssohn, 2012; Mahmoudi, 2013; Romero et al., 2015; Turner et al., 2014; Valentine et al., 2014). Also, Brooks et al. (2015) found no evidence of mixing or bioturbation in the surface layers of cores collected in the deep-sea area after the spill. In the deep-sea area, Chanton et al. (2015) demonstrated that the surface layer (0–1 cm) of some sites up to a distance of ~120 km from the DWH site contains significant amounts of DWH-derived petrocarbons. In addition, a detailed forensic study (Stout et al., 2016a) using the same publicly available data, demonstrated that the surface sediment layer (0–1 cm) of some sites located up to ~40 km from the DWH site, contains significant higher amounts of DWH oil than downcore sediment layers in recently contaminated sites containing background hydrocarbons or seep-derived hydrocarbons. Also, this study found that about 25% of the cores studied did not contain DWH oil, similar to our results in the deep-sea area (Section 3.1). In coastal areas, there were only 39 whole cores available in the databases, so the residual concentration of hydrocarbons was calculated based on the average concentration of hydrocarbons in the submerged layers from eight distinct subareas (Supplementary Table 3). The surface layer was also evaluated for oil content and specifically for DWH oil presence, using diagnostic ratios and hopane-normalized distributions of PAHs and biomarkers (Section 2.1.3), and only recently contaminated sites were included in the calculation of hydrocarbons deposition (Section 2.2.2) and degradation modeling (Section 2.3.2).

Given the presence of multiple hydrocarbon sources in the GoM (e.g. abundant and scatter natural seeps), large variability of background hydrocarbon concentrations (e.g. riverine, industry), and the DWH event that spilled approximately 7-times the average annual input of oil into the Gulf of Mexico (GoM) (MacDonald et al., 2015; Murawski et al., 2014; Stout et al., 2016a), we calculated the residual hydrocarbon concentration in the surface sediments to correct for background inputs (e.g. terrestrial, natural seeps). Stout et al. (2016a) showed that many sites in the deep-sea area contain both DWH and seep oil on the surface layer of the sediment cores. By calculating the residual hydrocarbon concentration within each sediment core (hydrocarbon concentration difference between the surface layer and downcore layers), the net deposition of oil-derived hydrocarbons post-spill is calculated. For example, in cases where recent deposition of oil-derived hydrocarbons was lower than seeps inputs (as indicated by downcore layers; e.g. MC338 area in Stout et al., 2016a), the residual concentration was <0 and not considered contaminated by the DWH spill. A different scenario was observed when recent deposition of oil-derived hydrocarbons was higher than seeps inputs (e.g. MC118 area in Stout et al., 2016a), the residual concentration was >0 and considered contaminated after the DWH spill and corrected by the background concentration. The samples with residual hydrocarbons >0 were further evaluated to distinguish DWH oil from other hydrocarbon sources in the GoM (see 2.1.3. Hydrocarbon diagnostic ratios).

In summary, there are three advantages for calculating residual

hydrocarbons as we did: first, it corrects for any possible variability among cores (sites) due to processing and analysis by multiple laboratories; second, it corrects for spatial variability in the concentration of hydrocarbons in the GoM previous to the DWH spill; and third, it corrects for other hydrocarbon sources present in 2010–2011 such as seeps and terrestrial (Conti et al., 2016; MacDonald et al., 2015; Stout et al., 2016a).

2.1.3. Hydrocarbon diagnostic ratios

Selected diagnostic ratios were calculated to assess the source and weathering of hydrocarbons in the sediment samples by study area (coastal, continental shelf, and deep-sea) and sedimentary layers (Section 2.3). To distinguish oil-derived hydrocarbons and DWH oil from multiple sources in the GoM (e.g. Mississippi River, seeps, petroleum industry, Taylor spill), hydrocarbon sources in the samples were evaluated using: 1) the Carbon Preference Index (CPI; $\sum$odd *n*-alkanes/$\sum$even *n*-alkanes for C_{10-40}); 2) TS/TM biomarker ratio (18α(H)-22,29,30-tris-norneohopane/17α(H)-22,29,30-trisnorhopane); 3) pyrogenic index (PI; $\sum$(other 3–6 ring EPA priority PAHs)/$\sum$(5 alkylated PAHs); 4) relative abundance of retene (Retene/Total PAHs × 100); and 5) and trends in observed hopane (17α(H),21β(H))-normalized distributions of PAHs in sediment samples relative to the DWH oil (Aeppli et al., 2014; Mulabagal et al., 2013; Romero et al., 2015; Stout et al., 2016a; Wang and Fingas, 2003). For the pyrogenic index, the five alkylated PAHs are the alkylated compounds of: naphthalene, phenanthrene, dibenzothiophene, fluorene, and chrysene. The "other" 3–6 ring EPA priority PAHs are: biphenyl, acenaphthylene, acenaphthene, anthracene, fluoranthene, pyrene, benz(*a*)anthracene, benzo(*b*)fluoranthene, benzo(k)fluoranthene, benzo(e)pyrene, benzo(*a*)pyrene, perylene, indeno(1,2,3-*c*,*d*)pyrene, dibenz(a,h) anthrance, and benzo(ghi)perylene. To compare samples with the DWH oil, the hydrocarbon composition of the DWH oil (source oil: MC252) was obtained from the BP Gulf Coast Restoration Organization (http://gulfsciencedata.bp.com/).

Weathering of hydrocarbon compounds in the sediment samples was studied using the ratios of *n*-alkane C17/pristane, low molecular weight PAHs to high molecular weight PAHs (2–3 rings/4–6 rings), relative abundance of Chrysene (Chrysene/Total PAHs × 100), and relative abundance of triaromatic steroids (TAS-C_{26-28}/Total biomarkers × 100) (Aeppli et al., 2014; Romero et al., 2015; Wang and Fingas, 2003; Yunker and Macdonald, 2003).

2.2. Large-scale spatial analysis

2.2.1. Spatial modeling

Residual hydrocarbons concentration data (surface layer minus downcore-background concentration) from 2,613 stations covering coastal, continental shelf and deep-sea areas, were included in the geostatistical analysis to generate a spatial distribution map. The spatial extent was limited by the shoreline (http://shoreline.noaa.gov/data/datasheets/composite.html; NOAA composite shoreline at mean tidal high water), the bathymetry line at 200 m depth (http://www.gebco.net/; GEBCO: Bathymetric Chart of the Oceans), and geographic extension of the study sites beyond 200 m depth. Specifically, data were imported in ArcGIS 10.3 (ESRI, Redlands, CA, USA) and interpolated with the Empirical Bayesian Kriging (EBK) method available from the Geostatistical Analyst Toolbox. EBK analysis is a geostatistical interpolation technique that uses the measured data to develop a statistical semivariogram model for prediction of surface values (Krivoruchko, 2012). It is a robust analysis that has been previously used to study contamination in the environment (Chanton et al., 2015; Pandey et al., 2015; Valentine et al., 2014). Several input parameters for the geostatistical interpolation were adjusted to improve computational efficiency and statistical fit of the model (Supplementary Table 4). In addition, due to the variable density of sites (as the result of non-random sampling conducted during the environmental impact surveys; Stout et al., 2016b) and hydrocarbon concentrations (non-uniform deposition of contaminated particles; Stout and Payne, 2016b) in the large area covered in our study (194,112 km^2), we tested the statistical performance of the model covering the full studied area and the performance of specific areas in the GoM separately (coastal, continental shelf, deep-sea). Results of this test (Supplementary Table 4) indicate that the spatial model performance is not affected by density of sampling sites and areas. The distribution of residual hydrocarbons obtained with the geostatistical model was also compared with bottom drainage paths in direction down-slope using drainage data from the Gulf of Mexico Coastal Ocean Observing System (GCOOS) data portal (http://gcoos.tamu.edu/products/topography/Shapefiles.html). Coastal relief model data from GCOOS was used to calculate seafloor slope and drainage direction in the area of interest using ArcGIS 10.3 (Spatial Analyst Toolbox \ Hydrology Toolset).

2.2.2. Calculation of hydrocarbons deposition

To estimate the total deposition of hydrocarbons post-spill in the GoM, we first calculated the cumulative area per range of residual hydrocarbon concentration using Empirical Bayesian Kriging analysis (see details in the previous section). For each range of residual hydrocarbon concentration, we multiplied the cumulative area by the average concentration (±CI) of residual hydrocarbons, the sediment surface interval, and by the average of surface sediment bulk density for the GoM (deep areas: 0.38 ± 0.16 g/cm^3, shallow areas: 0.69 ± 0.21 g/cm^3) (Burdige, 2006; Rowe and Kennicutt II, 2009; Valentine et al., 2014). Then, we added these results to yield the total deposition of hydrocarbons in the GoM (in metric tons). This value was compared to the amount of >C9 hydrocarbons (saturated and aromatic fractions calculated by Reddy et al., 2011a) discharged from the DWH spill after recovering efforts (87,752 metric tons >C9 hydrocarbons). Our calculation produced a lower limit of the total discharge of hydrocarbons post-spill due to three limitations. First, we used a very conservative thickness of the surface layer (0–2 cm for the coastal area, 0–2 cm for the continental shelf area, and 0–1 cm for the deep-sea area). Contamination was observed down to 5 cm depth in the sediments in large coastal areas (DWH Trustees, 2015; Lin and Mendelssohn, 2012; Mahmoudi, 2013; Turner et al., 2014) and in some limited deep-sea areas (Joye et al., 2014; Stout et al., 2016a). Second, a limited number of sites in some locations, for example in the continental shelf in Florida and Texas, and areas deeper than 2600 m depth. Third, our calculations do not correct for transformation processes of the most degradable hydrocarbon compounds (e.g. C10-20 *n*-alkanes) after deposition.

2.3. Fate of deposited hydrocarbons

2.3.1. Time-series data

Sediment cores were collected from 2010 to 2013 at three sediment-coring sites located at the DeSoto Canyon (28.59°N–87.53°W; 29.07°N–87.52°W; 29.06°N–87.16°W). The collection method and geochemical analyses of the sediment cores from the DeSoto Canyon are described in detail in Romero et al. (2015). We integrated geochemical and geochronology data to detect the sedimentary layer deposited in 2010 over time in the DeSoto Canyon cores (buried into deeper depths). The depth of the sedimentary layer corresponding to 2010 ± 0.8 was identified in each core and subsequently used for hydrocarbon analyses (Supplementary Tables 5, 6, 7; Brooks et al., 2015). This 2010-layer was identified using short-lived radioisotope measurements (^{210}Pb)

and a geochronological model in our time-series study following the methods in Brooks et al., 2015. Specifically, samples were analyzed by gamma spectrometry on Canberra HPGe (High-Purity Germanium) Coaxial Planar Photon Detectors for total ^{210}Pb (46.5Kev), ^{214}Pb (295 Kev and 351 Kev), and ^{214}Bi (609Kev) activities. Data were corrected for counting time and detector efficiency, as well as for the fraction of the total radioisotope measured yielding activity in dpm g^{-1} (disintegrations per minute per gram). Detection limits were all <3% of activities measured, determined by similar methods (Kitto, 1991). Efficiency calibrations were based on analyzing 12 varying masses (1–50 g) of the IAEA-447 organic standard. The Constant Rate of Supply (CRS) model was employed to assign specific ages to sedimentary layers, which is the most appropriate age model for systems with variable accumulation rates (Appleby and Oldfield, 1983; Binford, 1990).

2.3.2. Degradation modeling

Previous studies have demonstrated DWH oil was partitioned into dissolved, evaporated, and undissolved hydrocarbons mixtures along different transport pathways following the release into the GoM (Ryerson et al., 2012) and before deposition on the seafloor (Romero et al., 2015; Stout and Payne, 2016b). In the present study, we investigate the potential persistence in the sedimentary environment of the weathered hydrocarbons that were deposited following the DWH spill. The persistence of weathered hydrocarbons in sediments is controlled by post-depositional processes (e.g. biodegradation) depending primarily on the chemical properties of the compound groups (e.g. solubility of aliphatics, aromatics, biomarkers) and *in situ* temperature (Radović et al., 2014; Tansel et al., 2011). Highly variable environmental conditions in the GoM (e.g. temperature: 4–24 °C), primarily due to bathymetry (<20 m–>3000 m) affect biodegradation rate patterns at a large spatial scale (Louvado et al., 2015; Tansel et al., 2011). Taking into account these parameters, we estimated the concentration of hydrocarbon compounds for a period of 10 years after 2010. The persistence of hydrocarbons after deposition was studied by estimating the concentration of specific compound groups over time based on a large-scale degradation model from shallow to deep areas in the Gulf of Mexico (Tansel et al., 2011). The degradation model assumes (1) degradation follows first order kinetics, (2) half-lives vary among chemical structure of compounds, and (3) degradation of specific compounds depends primarily on water and sediment temperature. The model was extended to include all compound groups in our study using degradation rate constants from Wardlaw et al. (2011) and corrected for temperature effect (Tansel et al., 2011). Large-scale degradation models are limited by local half-lives of specific compounds influenced by factors such as nutrients and oxygen, and interactions between microbial communities and geochemical parameters that affect degradation rates (Arndt et al., 2013; Gong et al., 2014; Mahmoudi, 2013; Mason et al., 2012; Ziervogel et al., 2015). Due to these limitations of the model, we tested the degradation model in the deep-sea area, where we compared the data generated from the degradation model with *in situ* data collected in our time-series sites in the DeSoto Canyon from 2010 to 2013. Only *in situ* data from the sedimentary layer deposited in 2010 was used. Our results indicate good agreement between the model and *in situ* data (Section 3.3.) therefore, we extended the model to the deep-sea, continental-shelf, and coastal areas and compared results with other *in situ* studies .

3. Results and discussion

3.1. Temporal and spatial patterns

Comparative analysis of sedimentary layers in recently contaminated sediments (methods in Section 2.3) reveals a strong temporal change from pre-to post-spill in hydrocarbon concentrations. A 4- to 30-fold increase in ∑Hydrocarbons (sum of >C9 hydrocarbons) was observed in the post-spill surface layer compared to downcore pre-spill sediment layers in deep-sea ($p < 0.001$, 84% of total deep-sea sites) and coastal ($p < 0.01$, 60% of total coastal sites) areas of the northern GoM (Fig. 1). This trend was observed for more recalcitrant compounds like biomarkers (hopanoids, steranes, triaromatic steroids, $p < 0.01$), as well as for more degradable compounds like *n*-alkanes (C_{10}–C_{40}, $p < 0.01$) (Table 1). A significant 3-fold increase in PAH concentration was observed in the surface layer compared to downcore pre-spill sediment layers ($p < 0.01$) only in the deep-sea area, where low-molecular weight (LMW) PAHs were entrained in the submerged deep plume (McNutt et al., 2012b; Ryerson et al., 2012) and a fraction deposited on the seafloor (Daly et al., 2016; Romero et al., 2015). In addition, the coastal area showed that the post-spill sedimentary layer contains the highest concentrations of biomarker and *n*-alkane compounds, while PAH concentrations were the highest in the deep-sea area (Table 1).

Hydrocarbon sources were also distinct in recently contaminated sediments (post-spill sedimentary layer) in coastal and deep-sea areas. Specifically, diagnostic ratios of hopanes and *n*-alkanes in the post-spill layer indicate larger petrogenic inputs (CPI ratio; $p < 0.001$; Fig. 2) and DWH oil (TS/TM ratio; $p < 0.001$; Fig. 2). Also, preference biodegradation was observed for T7-T10 (C28–C29 tricyclic terpanes), T32-T35 (tetrakishomohopane and pentakishomohopane terpanes), and S4, S5, S14, S15 (13B(H),17A(H)–20S + R-diacholestane and 14B(H),17B(H)–20S + R-cholestane) (Supplementary Fig. 2), characteristic of DWH weathered oil deposited on the seafloor (Stout and Payne, 2016b). Diagnostic ratios of PAHs in the post-spill layer of contaminated sites indicate recent deposition of petrogenic inputs (PI ratio; $p < 0.001$; Fig. 2) only in the deep-sea area. There was no significant change in the PI ratio between the pre- and post-spill layers in the coastal area ($p > 0.05$); while a significant change ($p < 0.001$) to weathered/pyrogenic inputs in the surface layer was observed in the continental shelf area (Fig. 2). This PI ratio trend is attributed by the combined

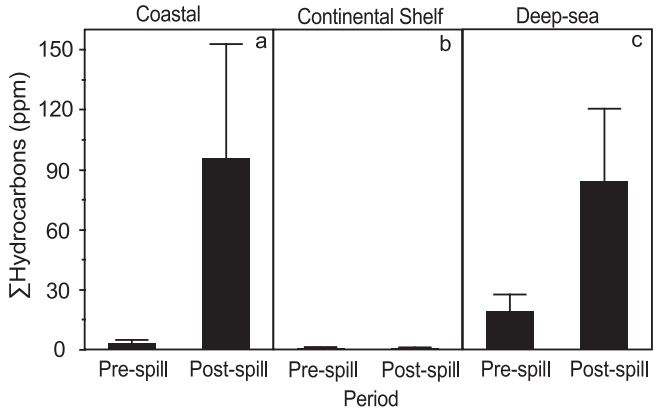

Fig. 1. Temporal change in ∑Hydrocarbons from sediment cores collected after the Deepwater Horizon spill. Data shown as mean ± 95% confidence interval in a) coastal (including bays and estuaries to 15 km out of the coastline), b) continental shelf (extending from 15 km out of the coastline to the 200 m water-column depth), and c) deep-sea (from 200 to 2600 m water-column depth) areas in the Gulf of Mexico. ∑Hydrocarbons refer to the sum of >C9 hydrocarbons (aliphatics: *n*-alkanes $C_{10\text{-}40}$, isoprenoids, branched alkanes; polycyclic aromatic: 2–6 ring, including alkylated homologues; hopanoids: $C_{27\text{-}35}$; steranes: $C_{27\text{-}29}$; triaromatic steroids: $C_{26\text{-}28}$). Sediment cores were collected in 2010–2011 (Supplementary Table 1). Post-spill denotes hydrocarbon concentration in the surface layer, and pre-spill indicates concentration in downcore layers (background) of the sediment cores analyzed.

Table 1
Concentrations (ppm) as mean ± 95% confidence interval (CI) of ∑Hydrocarbons (sum of >C9 hydrocarbons), PAHs (polycyclic aromatic hydrocarbons: 2–6 rings and alkylated homologues), *n*-alkanes (C_{10-40}), and biomarkers (hopanoids: C_{27-35}, steranes: C_{27-29}, and triaromatic steroids: C_{26-28}). Data shown for the surface (post-spill) and downcore (pre-spill) layers of sediment cores collected from coastal, continental shelf and deep-sea areas in the Gulf of Mexico.

Area	Sediment Layer	ΣHydrocarbons		PAHs		*n*-alkanes		Biomarkers	
		Mean	CI	Mean	CI	Mean	CI	Mean	CI
Coastal	Post-spill	95.9 ± 56.8		1.00 ± 0.58		75.72 ± 47.56		10.21 ± 4.08	
	Pre-spill	3.1 ± 1.6		0.57 ± 0.48		1.55 ± 1.23		0.39 ± 0.20	
Continental Shelf	Post-spill	0.7 ± 0.2		0.11 ± 0.04		0.59 ± 0.19		0.07 ± 0.02	
	Pre-spill	1.0 ± 0.3		0.04 ± 0.01		0.73 ± 0.19		0.08 ± 0.01	
Deep-sea	Post-spill	80.6 ± 34.6		15.09 ± 6.67		47.73 ± 20.74		4.67 ± 1.31	
	Pre-spill	18.5 ± 7.8		3.76 ± 1.70		10.64 ± 4.64		1.24 ± 0.30	

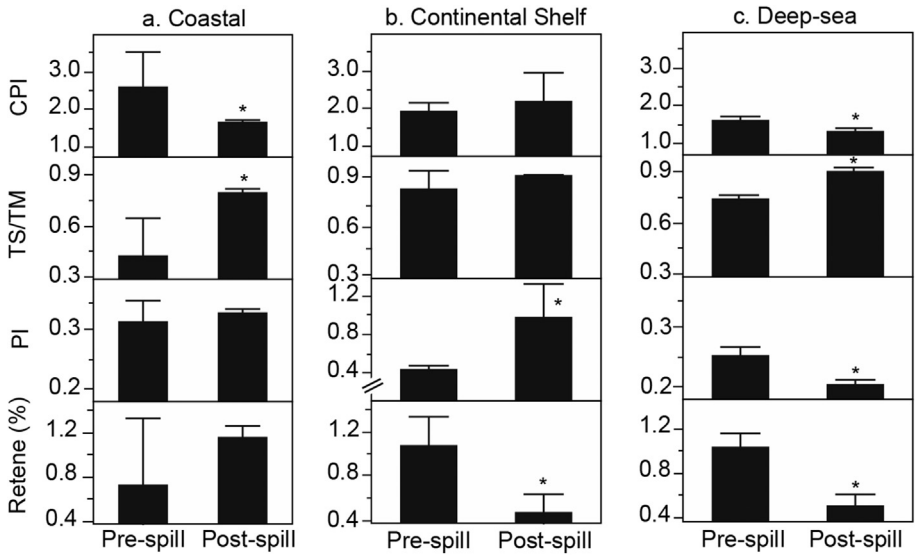

Fig. 2. Temporal changes in diagnostic source ratios from sediment cores collected after the Deepwater Horizon spill. Data shown as mean ± 95% confidence interval, in a) coastal (including bays and estuaries to 15 km out of the coastline), b) continental shelf (extending from 15 km out of the coastline to the 200 m water-column depth), and c) deep-sea (from 200 to 2600 m water-column depth) areas in the Gulf of Mexico. Post-spill denotes ratios from the surface sediment layer, and pre-spill indicates ratios from downcore layers from the cores analyzed, with CPI (Carbon preference index) = ∑odd Cn/∑even Cn; TS/TM = 18α(H)-22,29,30-tris-norneohopane/17α(H)-22,29,30-trisnorhopane; PI = ∑(other 3–6 ring EPA priority PAHs)/∑(5 alkylated PAHs); Retene (%) = Retene/Total PAHs × 100. Diagnostic ratios for DWH oil (Aeppli et al., 2014; Romero et al., 2015): CPI (0.9 ± 0.004), TS/TM (1.1 ± 0.2), PI (0.01 ± 0.03), Retene% (non-detectable). An asterisk (*) indicates significant changes ($P < 0.05$) in the post-spill layer relative to the pre-spill layer.

effects of multiple weathering processes (dissolution, evaporation, biodegradataion and photo-oxidation) during transport of DWH oil to the coastal area affecting the use of conventional diagnostic ratios for PAHs (Stout et al., 2015) and mixed with environmental PAHs (e.g. retene; Fig. 2). In the deep-sea area, about 50% of the contaminated sites with petrogenic PAHs denote mix inputs from DWH oil (dominated by C3–C4 benz(*a*)anthracenes/Chrysenes, and low perylene content; Supplementary Fig. 3), and natural seeps (abundant C2–C4 decalines, C2–C4 phenanthrenes, and C4 fluoranthenes/pyrens; Supplementary Fig. 3) as observed previously (Stout et al., 2016a). This is not surprising due to the relatively high annual input of hydrocarbons by natural seeps in the GoM (~95,500 tons of oil; Ocean Studies Board and Marine Board, 2003), covering extensive areas (MacDonald et al., 2015).

In non-contaminated sediments, 25% of the sites in the deep-sea and 40% in the costal area, have lower or similar ∑Hydrocarbon concentrations in the surface layer (post-spill) relative to downcore layers (pre-spill). Also, hydrocarbon sources in these sites are different from the DWH oil (Supplementary Table 8) in multiple sediment layers within a core. Hydrocarbon sources for the non-contaminated sediments are predominantly from biogenic sources (higher CPI ratio, retene, perylene, and T20 + T26 terpenes than recently contaminated sediments) and natural seeps (lower TS/TM ratio, and higher C2–C4 decalines and C2–C4 phenanthrenes than recently contaminated sediments) (Fig. 2, Supplementary Fig. 3, Supplementary Table 8). Biogenic inputs are primarily terrestrial from watershed runoff from the Atchafalaya and Mississippi Rivers and coastal plants debris that deposits within 30 km off the Mississippi River, and up to ~200 km from the Mississippi River delta (Gordon and Goñi, 2004; Kujau et al., 2010). Similar number of non-contaminated sites in the deep-sea area was also observed by Stout et al. (2016a).

The overall spatial trend in the composition of hydrocarbons matches previous observations of hydrocarbon mass flows in the environment (McNutt et al., 2012b; Reddy et al., 2011b; Ryerson et al., 2012). Transport of surface slicks rich in the heaviest hydrocarbons such as *n*-alkanes (C > 23) and biomarkers (Reddy et al., 2011b; Ryerson et al., 2012) to coastal areas, while more soluble hydrocarbons abundant in the water column and in submerged plumes from the DWH spill, such as PAHs (Reddy et al., 2011b; Ryerson et al., 2012), were transported to deeper benthic areas in the GoM (Daly et al., 2016; Romero et al., 2015). This is supported by the spatial trend of PAH concentrations and ratios (Table 1, Fig. 2), with weathered mixed PAHs in the coastal area (PI = 0.4 ± 0.02; retene = 2.1 ± 0.1%), pyrogenic PAHs in the continental shelf (PI = 0.8 ± 0.3; retene = 0.3 ± 0.2%), and dominant petrogenic inputs in the deep-sea (PI = 0.2 ± 0.02; retene = 0.6 ± 0.1%) relative to the DWH oil (Romero et al., 2015). Also, some sites (N = 26) in the

deep-sea showed a larger content of pyrogenic PAHs (PI > 0.5). It is likely that pyrogenic PAHs were derived from an incomplete combustion of large surface oil slicks that were burned during the response efforts to the DWH oil spill (~222,000–313,000 barrels) (Adhikari et al., 2016; McNutt et al., 2012b; Romero et al., 2015; Shigenaka et al., 2015; Stout and Payne, 2016a) and/or from intense weathering of oil slicks exposed to high summer temperatures (25–30 °C), which enhanced the evaporation of low molecular weight compounds (Aeppli et al., 2014; Bacosa et al., 2015; McNutt et al., 2012b; Romero et al., 2015; Ryerson et al., 2012).

3.2. Large-scale deposition

The base-scale analysis of residual hydrocarbons (surface layer minus downcore-background concentration) suggests that following the DWH spill, contamination in sediments (residual hydrocarbon concentration >0) was observed up to a distance of 180 km from the DWH rig in the deep-sea area, and up to 517 km in coastal and continental shelf areas (Fig. 3). The spatial distribution of residual hydrocarbons (Fig. 4) agrees with visually impacted regions reported for coastal areas in Louisiana (e.g. Barataria Bay, Chandeleur Islands), Mississippi (e.g. Horn and Petit Bois Islands), Alabama (e.g. Cat Island), and Florida (e.g. Panhandle area) (DWH Trustees, 2015; Floyd et al., 2012), and for offshore deep-sea areas (e.g. Mississippi Canyon, DeSoto Canyon) (Brooks et al., 2015; Chanton et al., 2015; Stout et al., 2016b; Valentine et al., 2014). Further, the geostatistical model generated using the residual hydrocarbon data (Fig. 4) agrees with the actual values observed in the study area (Fig. 4) and impacted regions reported in the GoM (Chanton et al., 2015; DWH Trustees, 2015; Floyd et al., 2012; Valentine et al., 2014; Stout et al., 2016a, b).

A distinct spatial distribution of both hydrocarbon residual concentrations (Fig. 4) and weathering indicator ratios (Supplementary Fig. 4) denotes that the deposition on surface sediments occurred via various transport mechanisms due to partitioning of petroleum hydrocarbons at depth into aqueous, gas and particulate phases (Reddy et al., 2011b; Ryerson et al., 2012), as suggested elsewhere (Brooks et al., 2015; Chanton et al., 2015; Romero et al., 2015; Valentine et al., 2014). Specifically, before deposition surface slicks were transported along the Louisiana-Texas coastline region by sustained downwelling favorable winds combined with high Mississippi River discharges and river induced stratification (Kourafalou and Androulidakis, 2013). In contrast, anticyclonic circulation in the region east of the Mississippi Delta created a front, which restrained onshore transport of surface slicks (Kourafalou and Androulidakis, 2013). The spatial model indicates that high concentration of hydrocarbons deposited on ~4% of the contaminated coastal area (>10 ppm; Fig. 4 and Supplementary Fig. 4) containing weathered hydrocarbons (nC17/Pr <3.0, Chry >12%, HMW/LMW >3.0, TAS >16%) due to degradation, dissolution and/or photo-oxidation processes during horizontal transport of surface slicks towards the coast (Aeppli et al., 2012; Ryerson et al., 2012; Stout and Payne, 2016a). Less weathered oil at lower concentrations were deposited in ~97% of the contaminated shallow areas (<10 ppm; Fig. 4 and Supplementary Fig. 4) with settling of oil-mineral aggregates from the water column as a probably source, in areas where contamination was observed (Murawski et al., 2016; Wade et al., 2016). Also, a large phytoplankton bloom (>11,000 km^2) covering the continental shelf and slope east of the Mississippi Delta (O'Connor et al., 2016) may have contributed to the weathering of hydrocarbons in the water column subsequently reducing deposition of hydrocarbons in this area (Fig. 4). In the deep-sea, hydrocarbon deposition was greater at 1,300–1,600 m depth up to 30 km from the DWH rig and at 1,000–1,300 m depth from 30 km to 175 km from the DWH rig (Fig. 4) following the trajectory of the seafloor and submerged plumes, respectively (Camilli et al., 2010; Chanton et al., 2015; Daly et al., 2016). Deposited hydrocarbons at high concentrations (>50 ppm; Supplementary Fig. 4) were observed in only ~1.0% of the deep-sea area containing heavy weathered alkanes (nC17/Pr < 0.4) and LMW PAHs (HMW/LMW >1.0), possibly from settling of oil-mineral aggregates from the surface column-water observed close to the DWH site (Daly et al., 2016). In contrast, hydrocarbons (>C9 saturated and aromatic fractions) deposited in most of the deep-sea area contain lower concentrations of ∑hydrocarbons (<50 ppm; Supplementary Fig. 4) with weathered HMW PAHs (Chry >1.0%) and high relative abundance of LMW PAHs, possibly from settling of oil-mineral aggregates from the submerged plumes (Daly et al., 2016; Romero et al., 2015; Ryerson et al., 2012). The spatial trends observed following the trajectory of the seafloor and submerged plumes predominantly in southwest direction (Fig. 4,

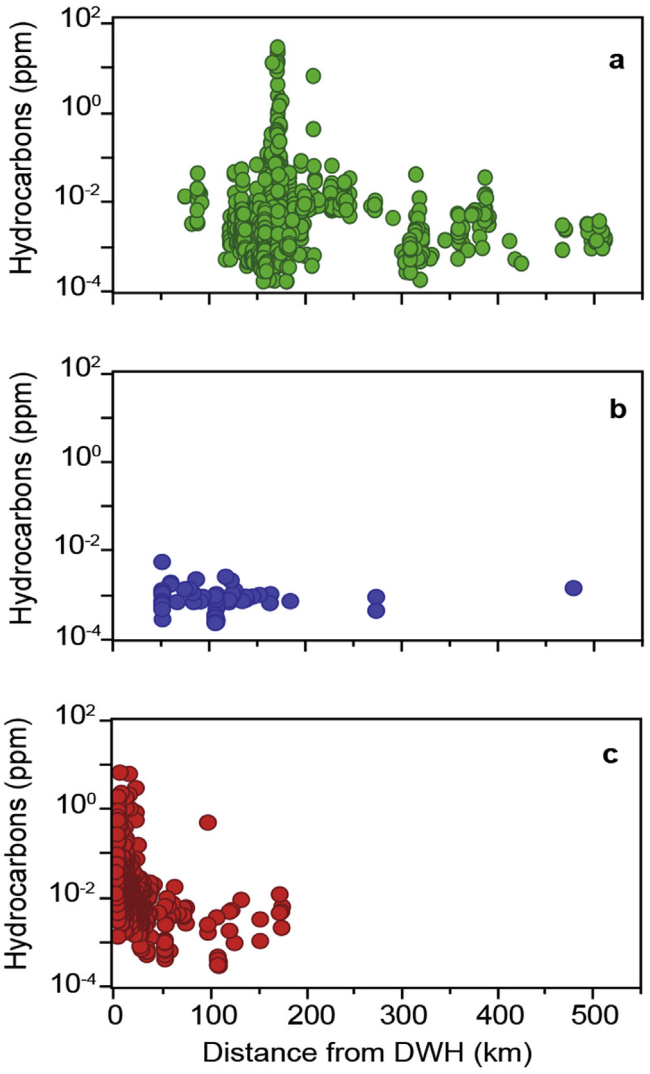

Fig. 3. Spatial extent of contaminated sediments found in the northern Gulf of Mexico after the Deepwater Horizon spill. Data shown for a) coastal, b) continental shelf, and c) deep-sea areas. Contaminated sediments contain higher ∑Hydrocarbons in the surface layer (post-spill) compared to downcore layers (background, pre-spill) of the sediment cores analyzed. Sediment cores were collected in 2010–2011 (Supplementary Table 1). ∑Hydrocarbons refer to the sum of aliphatics (*n*-alkanes C_{10-40}, isoprenoids, branched alkanes), polycyclic aromatic (2–6 ring, including alkylated homologues), hopanoid (C_{27-35}), sterane (C_{27-29}) and triaromatic steroid (C_{26-28}) compounds.

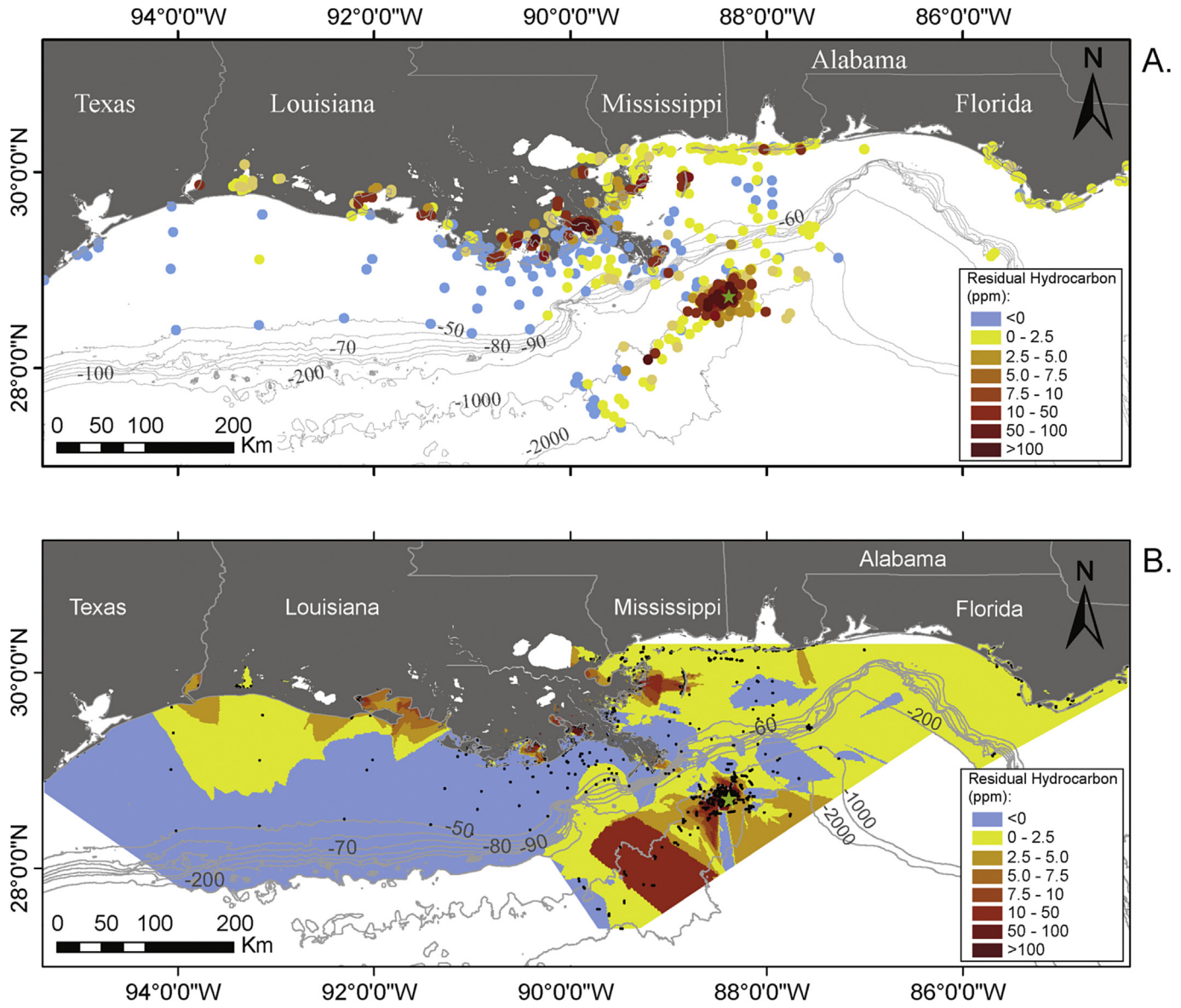

Fig. 4. Residual hydrocarbon concentrations (ppm) in surface sediments after the Deepwater Horizon spill in the Gulf of Mexico. A) Residual hydrocarbon concentrations at each study site from coastal to deep-sea areas. B) Spatial distribution model of residual hydrocarbon concentrations from coastal to deep-sea areas. Data was interpolated using Empirical Bayesian Kriging (EBK) analysis to calculate cumulative areal extent for each concentration range from Table 2. Input parameters for the EBK model for the full area are in Supplementary Table 3. Sediment cores (N = 2,613) were collected in 2010–2011 (Supplementary Table 1). Residual hydrocarbons refer to surface layer minus background concentration. Hydrocarbon concentrations include the sum of aliphatics (*n*-alkanes C_{10-40}, isoprenoids, branched alkanes), polycyclic aromatic (2–6 ring, including alkylated homologues), hopanoid (C_{27-35}), sterane (C_{27-29}) and triaromatic steroid (C_{26-28}) compounds. Gray lines indicate bathymetry (m). Green star: location of the DWH site. (For interpretation of the colour concentration ranges in this figure legend, the reader is referred to the web version of this article.)

Supplementary Fig. 4), indicate that the weathering of oil occurred principally before deposition on the seafloor, and was affected mostly by dissolution and biodegradation in the submerged plumes and during vertical transport to the seafloor (Stout and Payne, 2016b).

Results also indicate that a total cumulative area of ~110,000 km^2 was contaminated post-spill, with a total hydrocarbon input to surface sediments (background subtracted) of $1.9 \pm 0.9 \times 10^4$ metric tons (up to 4.1×10^4 metric tons) of oil-derived hydrocarbons (>C9 saturated and aromatic fractions) (Table 2), equivalent to the deposition of about $9.1 \pm 4.1 \times 10^4$ metric tons of DWH crude oil. The total deposition of hydrocarbons to surface sediments corresponds to 21 ± 10% (up to 47%) of the total amount of oil discharged from the DWH spill that remained in the environment after recovery from the environment during response efforts (3.2 millions barrels; U.S. District Court, 2015). Specifically for each of the studied areas and relative to the oil mass that remained in the environment, 18.9± 9.8% (up to 43%) was deposited in the coastal area, 0.4± 0.1% (up to 0.5%) in the continental shelf area, and 2.0± 0.5% (up to 3.7%) in the deep-sea area. While our calculations yielded a conservative assessment of the amount of oil-derived hydrocarbons deposited on the seafloor, our estimates are within the bounds of the oil budget (McNutt et al., 2012a, b).

Specifically to the deep-sea, our calculations of the total mass of DWH oil deposited in this area using >C9 hydrocarbons in surface sediments, are within the range or close to previous studies using different methods, such as: ^{14}C data in surface sediments (3.0–4.9%

Table 2
Residual hydrocarbon concentrations, cumulative contaminated area, and total deposition of hydrocarbons to surface sediments in the Gulf of Mexico. Areas for each range of residual hydrocarbon concentration were calculated using Empirical Bayesian Kriging analysis. Residual hydrocarbons refer to surface layer concentration minus background concentration. Data shown as mean ± 95% confidence interval.

Area		Residual Hydrocarbon (ppm)			Area	Total deposition (tons)[b]	
		Average ± CI	min	max	(km^2)	Average (range)	
Coastal		1.0 ± 0.1	0.01	2.5	22,383	298	(282–471)
		3.6 ± 0.1	2.5	5.0	5,698	283	(275–438)
		6.1 ± 0.2	5.0	7.3	3,098	259	(251–399)
		8.5 ± 0.2	7.5	9.7	1,435	168	(164–260)
		23.6 ± 2.3	10.1	49.8	879	286	(258–471)
		74.4 ± 5.5	53.5	98.9	25	26	(24–42)
		4,075.1 ± 2,273.3	104.0	30,059.9	271	15,217	(6,729–35,560)
	Total				***33,789***	***16,538***	***(7,982–37,641)***
Continental Shelf		0.5 ± 0.1	0.1	1.3	42,068	274	(240–340)
		3.0 ± 0.7	2.6	3.4	1,007	41	(32–51)
		6.0[a]	*N.A.*	*N.A.*	29	2	*N.A. N.A.*
		8.5[a]	*N.A.*	*N.A.*	17	2	*N.A. N.A.*
	Total				***43,121***	***319***	***(277–395)***
Deep-sea		1.0 ± 0.1	0.01	2.5	17,623	69	(61–115)
		3.6 ± 0.2	2.5	4.9	6,228	85	(81–133)
		6.1 ± 0.2	5.0	7.5	475	11	(11–17)
		8.7 ± 0.2	7.6	9.9	418	14	(13–21)
		21.1 ± 1.5	10.0	48.4	7,610	609	(566–978)
		69.0 ± 8.3	54.0	93.4	76	20	(17–33)
		1,080.7 ± 456.4	123.7	6,010.4	219	898	(519–1,916)
	Total				***32,648***	***1 ,706***	***(1,269–3,213)***

[a] Concentration determined by the Kriging model.
[b] Total deposition (metric tons) = Area * sediment interval * sediment mass * residual hydrocarbon.

of the discharge oil; Chanton et al., 2015), 17α(H),21β(H)-hopane concentration in surface sediments (2.3–11.3% of the discharge oil; Valentine et al., 2014), and 17α(H),21β(H)-hopane concentration in 0–3 cm sedimentary layer (6.9–7.7% of the discharge oil; Stout et al., 2016b). Comparable spatial patterns were observed among the studies, indicating that the deposition of DWH oil was spatially heterogeneous, with larger inputs close to the DWH site. The differences observed among these studies in relation to the amount of DWH oil deposited in deep-sea floor, is attributed to the number of compounds used (one compound like 17α(H),21β(H)-hopane, instead of numerous hydrocarbon compounds including >C9 saturated and aromatic fractions) and the background correction applied (averaged background value instead of background value within each sediment core studied). The former is critical due to the partitioning of petroleum hydrocarbons at depth into aqueous, gas and particulate phases during the DWH spill (Reddy et al., 2011b; Ryerson et al., 2012) influencing the footprint at depth (Chanton et al., 2015; Romero et al., 2015; Stout et al., 2016b). Our impacted deep-sea area by the deposition of DWH oil is larger than these studies, however it is less than half of the total spatial extention calculated for the deep-plume (Du and Kessler, 2012). In addition, due to a sustained deposition of DWH oil of at least 5 months after the well was capped, it is plausible that DWH oil would have distributed to a wider area before deposition (Yan et al., 2016).

3.3. Significance for long-term fate

A fundamental requirement examining impacts of oil in natural environments, is to determine not only the concentration of hydrocarbons in sediments but also how the concentration and composition of hydrocarbons changes over time (Turner et al., 2014). Results in our study indicate that a large amount of hydrocarbons were deposited post-spill mostly in selected coastal and deep-sea areas (Figs. 1 and 4). Hydrocarbons deposited in these areas were different in amount, composition and degree of weathering (Supplementary Figs. 2, 3, 4) due to different vertical and horizontal transport mechanisms (Camilli et al., 2010; Daly et al., 2016; Kourafalou and Androulidakis, 2013; Reddy et al., 2011b; Romero et al., 2015; Ryerson et al., 2012; Stout and Payne, 2016b). We hypothesize that the long-term fate of the hydrocarbons deposited on the seafloor in the GoM following the DWH spill may not only depend on *in situ* transformation processes but also on redistribution of deposited hydrocarbons.

In the coastal area, a rapid degradation of LMW PAHs compounds in oiled sand-patties occurred within 19 months after the DWH spill (Gros et al., 2014). Similarly, in saltmarshes, dominance of HMW PAH compounds was observed after 24 months, indicating a possible long-term persistence of hydrocarbon compounds of at least a decade (Turner et al., 2014), as observed elsewhere (Reddy et al., 2002) and in our long-term estimates using the large-scale degradation model (Supplementary Fig. 5). The initial hydrocarbon composition of surface sediments from samples collected in 2010–2011 in the coastal and deep-sea areas was predominately *n*-alkanes ($C_{10\text{-}40}$) and 2–3 ring PAHs (~80%), which decreased to background concentrations in the following two years according to the model (Supplementary Figs. 5 and 6). Similar to previous studies in GoM coastal areas (Gros et al., 2014; Turner et al., 2014) the model estimated a long-term persistence of more recalcitrant compounds (e.g. biomarkers, HMW PAHs) (Supplementary Fig. 6). Also, a rapid decrease in concentration of more degradable hydrocarbons (e.g. PAHs, *n*-alkanes) was observed a year after the DWH spill, in our sedimentary collections at deep-sea sites in the DeSoto Canyon (Supplementary Fig. 7). The trend observed over time in the DeSoto Canyon (*in situ* time-series study) follows those from estimated concentrations in the same region ($p > 0.05$; Supplementary Fig. 7) and other studies in the GoM (Snyder et al., 2014) indicating a good performance of the degradation model. Some differences are observed between the two methods when comparing relative abundance of oil-derived hydrocarbons (Supplementary Fig. 8). Overall, results support the hypothesis of a long-term persistence (~decade) and potential impact from coastal to deep-sea environments of, not surprisingly, the most recalcitrant oil-derived hydrocarbons deposited in 2010–2011.

Redistribution of DWH oil residues deposited post-spill may as well affect the long-term fate of the most recalcitrant compounds in the sediments. Large-scale events in the GoM like hurricanes, can bring new contaminated sediments to coastal areas not impacted by the initial oiling in 2010 (Turner et al., 2014) and promote sediment resuspension and down-slope currents to deeper areas (Ross et al., 2009; Ziervogel et al., 2015). Also, natural heterogeneity of bottom topography and circulation processes may promote transport of materials to deeper areas in the GoM (Parinos et al., 2013; Ross et al., 2009) and elsewhere (e.g. Mediterranean Sea; Parinos et al., 2013). The combination of these processes has been observed in the Mississippi Canyon, where the net down-slope transport of bottom sediments is enhanced by hurricane activity, with variability in direction caused by canyon topography (Ross et al., 2009). Evidence of this transport to deeper areas in our study includes: (1) background (pre-spill) concentration trends (Fig. 1, Table 1) indicate that the deep-sea area serves as a repository system for hydrocarbons in the northern GoM, and (2) observations of regional-scale long transport and deposition to deeper areas (>1,500 m depth) of oil-associated marine snow from the DWH spill (Brooks et al., 2015; Daly et al., 2016; Passow et al., 2012; Chanton et al., 2015; Valentine et al., 2014). In our study, a gradient of residual hydrocarbons towards deeper depths was observed (>2,400 m; Fig. 4) along bottom drainage paths (Supplementary Fig. 9). Most of the samples in this area with the highest residual hydrocarbon concentrations (>5.0 ppm) were found at the highest slopes of morphological highs on the seafloor or on lower grade bottom drainage channels (Supplementary Fig. 9) where redistribution of sediments is expected. A recent study (Conti et al., 2016) describing high-resolution morphology of the seafloor about 5 km south-east of the DWH site, shows erosional channels indicative of high current speeds that are required to transport sediments and build this type of bottom morphology. Also in 2012, Hurricane Isaac induced resuspension of sedimentary organic matter in the Mississippi Canyon, redistributing deposited oil-derived hydrocarbons from the DWH spill (Ziervogel et al., 2015), possibly to deeper areas as observed in previous storm events in the northern GoM (Ross et al., 2009). These evidences suggest redistribution of deposited hydrocarbons should be consider as an important process for future modeling of long-term fate of oil-spills at depth.

4. Conclusion

We used a combination of analyses including geochemistry, geochronology, and spatial and degradation modeling to characterize the chemical signature, distribution, extent, and fate of the DWH oil deposited on the GoM seafloor in 2010–2011. A large number of chemical compounds (N = 158) and sediment cores (N = 2,613), and background correction within each core were included to take into account a large-spatial area (from coastal to deep-sea areas), the partitioning of hydrocarbons during transport in the water column, and hydrocarbon sources present in the GoM (e.g. biogenic, natural seeps). Results from this study, identify distinct weathered signatures for oil deposited in coastal and deep-sea areas related to hydrocarbon compounds specific chemical properties and transport mechanisms to the seafloor. The related spatial and chemical trends denote the complexity of chemical and physical processes transporting vertically and horizontally DWH oil in the GoM. Contamination (residual hydrocarbon >0) was observed in ~110,000 km^2, up to a distance of ~517 km from the DWH site. Diagnostic ratios and hopane-normalized distributions indicate surface sediments were contaminated with petrogenic hydrocarbons possible related to the DWH oil. Presence of other hydrocarbon sources was as well observed, primarily from natural seeps in the deep-sea area. Background corrected data (residual hydrocarbons) indicate that 21 ± 10% of the total amount of oil discharged and not recovered from the DWH spill may have been deposited on the seafloor, similar to the unaccounted amount reported previously (McNutt et al., 2012b). Sustained deposition of at least 5 months after the DWH well was capped (Yan et al., 2016), may have deposited even more DWH oil that remained in the environment, for a deposition up to 47% of the total amount of oil leaked and not recovered. The spatial and temporal trends indicate possible long-term persistence of the most recalcitrant hydrocarbon compounds deposited post-spill (~decade) and downslope redistribution to deeper areas.

Summary of main finding

21± 10% (up to 47%) of the total amount of oil discharged and not recovered from the Deepwater Horizon spill was found in ~110,000 km^2, from coastal to deep-sea areas in the Gulf of Mexico.

Acknowledgments

The authors would like to thank the crew of the R/V Weatherbird II for their help during the field program, and the technicians N. Zenzola, and G. Ellis for laboratory support. This research was made possible by a grant from The Gulf of Mexico Research Initiative (GOMRI) / C-IMAGE II (Center for Integrated Modeling and Analysis of the Gulf Ecosystem). Data are publicly available through the Gulf of Mexico Research Initiative & Data Cooperative (GRIIDC) at https://data.gulfresearchinitiative.org (doi:10.7266/N7ZG6Q71 and doi:10.7266/N7N29V16). Publicly data from ERMA Deepwater Gulf Response and British Petroleum Gulf Science are available online at https://gomex.erma.noaa.gov/, and http://gulfsciencedata.bp.com/, respectively.

Appendix A. Supplementary data

Supplementary data related to this article can be found at http://dx.doi.org/10.1016/j.envpol.2017.05.019.

References

Adhikari, P.L., Maiti, K., Overton, E.B., Rosenheim, B.E., Marx, B.D., 2016. Distributions and accumulation rates of polycyclic aromatic hydrocarbons in the northern Gulf of Mexico sediments. Environ. Pollut. 212, 413–423. http://dx.doi.org/10.1016/j.envpol.2016.01.064.

Aeppli, C., Carmichael, C.A., Nelson, R.K., Lemkau, K.L., Graham, W.M., Redmond, M.C., Valentine, D.L., Reddy, C.M., Graham, M., Redmond, M.C., Valentine, D.L., Reddy, C.M., 2012. Oil weathering after the Deepwater Horizon disaster led to the formation of oxygenated residues. Environ. Sci. Technol. 46, 8799–8807. http://dx.doi.org/10.1021/es3015138.

Aeppli, C., Nelson, R.K., Radović, J.R., Carmichael, C. a., Valentine, D.L., Reddy, C.M., 2014. Recalcitrance and degradation of petroleum biomarkers upon abiotic and biotic natural weathering of Deepwater Horizon oil. Environ. Sci. Technol. 48, 6726–6734. http://dx.doi.org/10.1021/es500825q.

Allan, S.E., Smith, B.W., Anderson, K. a, Brian, S.W., Anderson, K. a, 2012. Impact of the Deepwater Horizon oil spill on bio available polycyclic aromatic hydrocarbons in Gulf of Mexico coastal waters. Environ. Sci. Technol. 46, 2033–2039. http://dx.doi.org/10.1021/es202942q.

Appleby, P.G., Oldfield, F., 1983. The assessment of 210 Pb data from sites with varying sediment accumulation rates. Hydrobiologia 103, 29–35.

Arndt, S., Jørgensen, B.B., LaRowe, D.E., Middelburg, J.J., Pancost, R.D., Regnier, P., 2013. Quantifying the degradation of organic matter in marine sediments: a review and synthesis. Earth-Science Rev. 123, 53–86. http://dx.doi.org/10.1016/j.earscirev.2013.02.008.

Bacosa, H.P., Erdner, D.L., Liu, Z., 2015. Differentiating the roles of photooxidation and biodegradation in the weathering of Light Louisiana Sweet crude oil in surface water from the Deepwater Horizon site. Mar. Pollut. Bull. 95, 265–272. http://dx.doi.org/10.1016/j.marpolbul.2015.04.005.

Binford, M.W., 1990. Calculation and uncertainty analysis of 210Pb dates for PIRLA project lake sediment cores. J. Paleolimnol. 3, 253–267.

Brooks, G.R., Larson, R.A., Schwing, P.T., Romero, I., Moore, C., Reichart, G.J., Jilbert, T., Chanton, J.P., Hastings, D.W., Overholt, W.A., Marks, K.P., Kostka, J.E.,

Holmes, C.W., Hollander, D., 2015. Sedimentation pulse in the NE Gulf of Mexico following the 2010 DWH blowout. PLoS One 10, 1–24. http://dx.doi.org/10.1371/journal.pone.0132341.
Burdige, D.J., 2006. Geochemistry of Marine Sediments. Princeton University Press, Princeton. http://dx.doi.org/10.1086/533614.
8015C, E.M, 2007. Nonhalogenated Organics by Gas Chromatography, pp. 1–68.
Camilli, R., Reddy, C.M., Yoerger, D.R., Mooy, B.A.S., Van Jakuba, M.V., Kinsey, J.C., McIntyre, C.P., Sylva, S.P., Maloney, J.V., 2010. Tracking hydrocarbon plume transport and biodegradation at Deepwater Horizon. Sci. (80-.) 330, 201–204.
Chanton, J.P., Cherrier, J., Wilson, R.M., Sarkodee-Adoo, J., Bosman, S., Mickle, a, Graham, W.M., 2012. Radiocarbon evidence that carbon from the Deepwater Horizon spill entered the planktonic food web of the Gulf of Mexico. Environ. Res. Lett. 7, 45303. http://dx.doi.org/10.1088/1748-9326/7/4/045303.
Chanton, J., Zhao, T., Rosenheim, B.E., Joye, S., Bosman, S., Brunner, C., Yeager, K.M., Diercks, A.R., Hollander, D., 2015. Using natural abundance radiocarbon to trace the flux of petrocarbon to the seafloor following the Deepwater Horizon oil spill. Environ. Sci. Technol. 49, 847–854. http://dx.doi.org/10.1021/es5046524.
Conti, A., D'Emidio, M., Macelloni, L., Lutken, C., Asper, V., Woolsey, M., Jarnagin, R., Diercks, A., Highsmith, R.C., 2016. Morpho-acoustic characterization of natural seepage features near the Macondo Wellhead (ECOGIG site OC26, Gulf of Mexico). Deep. Res. Part II Top. Stud. Oceanogr. 129, 53–65. http://dx.doi.org/10.1016/j.dsr2.2015.11.011.
8270D, E.M, 2007. Semivolatile Organic Compounds by Gas Chromatography/Mass Spectrometry, pp. 1–72 (Gc/Ms).
Daly, K.L., Passow, U., Chanton, J., Hollander, D., 2016. Assessing the impacts of oil-associated marine snow formation and sedimentation during and after the Deepwater Horizon oil spill. Anthropocene 1–16. http://dx.doi.org/10.1016/j.ancene.2016.01.006.
Du, M., Kessler, J.D., 2012. Assessment of the spatial and temporal variability of bulk hydrocarbon respiration following the Deepwater Horizon oil spill. Environ. Sci. Technol. 46, 10499–10507. http://dx.doi.org/10.1021/es301363k.
DWH Trustees, 2015. Deepwater Horizon Oil Spill Draft Programmatic Damage Assessment and Restoration Plan and Draft Programmatic Environmental Impact Statement, pp. 1–685. http://www.gulfspillrestoration.noaa.gov/.
Floyd, E.L., Lungu, C.T., Gohlke, J.M., 2012. An Evaluation of Nearshore Sediment Data after the Deepwater Horizon Blowout, vol. 1, pp. 341–350.
Gong, Y., Zhao, X., Cai, Z., O'Reilly, S.E., Hao, X., Zhao, D., 2014. A review of oil, dispersed oil and sediment interactions in the aquatic environment: influence on the fate, transport and remediation of oil spills. Mar. Pollut. Bull. 79, 16–33. http://dx.doi.org/10.1016/j.marpolbul.2013.12.024.
Gordon, E.S., Goñi, M. a., 2004. Controls on the distribution and accumulation of terrigenous organic matter in sediments from the Mississippi and Atchafalaya river margin. Mar. Chem. 92, 331–352. http://dx.doi.org/10.1016/j.marchem.2004.06.035.
Gros, J., Reddy, C.M., Aeppli, C., Nelson, R.K., Carmichael, C.A., Arey, J.S., 2014. Resolving biodegradation patterns of persistent saturated hydrocarbons in weathered oil samples from the Deepwater Horizon disaster. Environ. Sci. Technol. 48, 1628–1637. http://dx.doi.org/10.1021/es4042836.
Harding, V., Camp, J., Morgan, L.J., Gryko, J., 2016. Oil residue contamination of continental shelf sediments of the Gulf of Mexico. Mar. Pollut. Bull. http://dx.doi.org/10.1016/j.marpolbul.2016.07.032.
Joye, S.B., Teske, A.P., Kostka, J.E., 2014. Microbial dynamics following the macondo oil well blowout across Gulf of Mexico environments. Bioscience 64, 766–777. http://dx.doi.org/10.1093/biosci/biu121.
Kitto, M.E., 1991. Determination of photon self-absorption corrections for soil samples. Int. J. Radiat. Appl. Instrum. Part A. Appl. Radiat. Isot. 42, 835–839.
Kourafalou, V.H., Androulidakis, Y.S., 2013. Influence of Mississippi River induced circulation on the Deepwater Horizon oil spill transport. J. Geophys. Res. Ocean. 118 http://dx.doi.org/10.1002/jgrc.20272 n/a-n/a.
Krivoruchko, K., 2012. Empirical Bayesian Kriging. ESRI Press Fall, pp. 6–10, 2012.
Kujau, A., Nürnberg, D., Zielhofer, C., Bahr, A., Röhl, U., 2010. Mississippi River discharge over the last ~560,000years — indications from X-ray fluorescence core-scanning. Palaeogeogr. Palaeoclimatol. Palaeoecol. 298, 311–318. http://dx.doi.org/10.1016/j.palaeo.2010.10.005.
Lin, Q., Mendelssohn, I.A., 2012. Impacts and recovery of the Deepwater Horizon oil spill on vegetation structure and function of coastal salt marshes in the northern Gulf of Mexico. Environ. Sci. Technol. 46, 3737–3743.
Louvado, A., Gomes, N.C.M., Simões, M.M.Q., Almeida, A., Cleary, D.F.R., Cunha, A., 2015. Polycyclic aromatic hydrocarbons in deep sea sediments : microbe – pollutant interactions in a remote environment. Sci. Total Environ. 526, 312–328. http://dx.doi.org/10.1016/j.scitotenv.2015.04.048.
MacDonald, I.R., Garcia-Pineda, O., Beet, A., Daneshgar, A., Feng, L., Graettinger, G., French-McCay, D., Holmes, J., Hu, C., Huffer, F., Leifer, I., Muller-Karger, F., Solow, A., Silva, M., Swayze, G., 2015. Natural and unnatural oil slicks in the Gulf of Mexico. J. Geophys. Res. Ocean. 120, 3896–3912. Doi:110.1002/2015JC011062.
Mahmoudi, N., 2013. Assessing *in situ* Degradation of Petroleum Hydrocarbons by Indigenous Microbial Communities. Open Access Dissertations and Theses, McMaster University. Paper 7882. 195 pages.
Mason, O.U., Hazen, T.C., Borglin, S., Chain, P.S.G., Dubinsky, E. a, Fortney, J.L., Han, J., Holman, H.-Y.N., Hultman, J., Lamendella, R., Mackelprang, R., Malfatti, S., Tom, L.M., Tringe, S.G., Woyke, T., Zhou, J., Rubin, E.M., Jansson, J.K., 2012. Metagenome, metatranscriptome and single-cell sequencing reveal microbial response to Deepwater Horizon oil spill. ISME J. 6, 1715–1727. http://dx.doi.org/10.1038/ismej.2012.59.
McNutt, M.K., Camilli, R., Crone, T.J., Guthrie, G.D., Hsieh, P. a, Ryerson, T.B., Savas, O., Shaffer, F., 2012a. Review of flow rate estimates of the Deepwater Horizon oil spill. Proc. Natl. Acad. Sci. U. S. A. 109, 20260–20267. http://dx.doi.org/10.1073/pnas.1112139108.
McNutt, M.K., Chu, S., Lubchenco, J., Hunter, T., Dreyfus, G., Murawski, S. a, Kennedy, D.M., 2012b. Applications of science and engineering to quantify and control the Deepwater Horizon oil spill. Proc. Natl. Acad. Sci. U. S. A. 109, 20222–20228. http://dx.doi.org/10.1073/pnas.1214389109.
Montagna, P. a, Baguley, J.G., Cooksey, C., Hartwell, I., Hyde, L.J., Hyland, J.L., Kalke, R.D., Kracker, L.M., Reuscher, M., Rhodes, A.C.E., 2013. Deep-sea benthic footprint of the Deepwater Horizon blowout. PLoS One 8, e70540. http://dx.doi.org/10.1371/journal.pone.0070540.
Mulabagal, V., Yin, F., John, G.F., Hayworth, J.S., Clement, T.P., 2013. Chemical fingerprinting of petroleum biomarkers in Deepwater Horizon oil spill samples collected from Alabama shoreline. Mar. Pollut. Bull. 70, 147–154. http://dx.doi.org/10.1016/j.marpolbul.2013.02.026.
Murawski, S.A., Hogarth, W.T., Peebles, E.B., Barbeiri, L., 2014. Prevalence of external skin lesions and polycyclic aromatic hydrocarbon concentrations in Gulf of of Mexico fishes. Post-Deepwater Horiz. Trans. Am. Fish. Soc. 143, 37–41. http://dx.doi.org/10.1080/00028487.2014.911205.
Murawski, S.A., Fleeger, J.W., Patterson III, W.F., Hu, C., Daly, K., Romero, I.C., Toro-Farmer, G.A., 2016. How did the Deepwater Horizon oil spill affect coastal and continental shelf ecosystems of the Gulf of Mexico? Oceanography 29.
Nixon, Z., Zengel, S., Baker, M., Steinhoff, M., Fricano, G., Rouhani, S., Michel, J., 2016. Shoreline oiling from the Deepwater Horizon oil spill. Mar. Pollut. Bull. 107, 170–178. http://dx.doi.org/10.1016/j.marpolbul.2016.04.003.
NRDA, 2011. Analytical Quality Assurance Plan Mississippi Canyon 252 (Deepwater Horizon).
Ocean Studies Board and Marine Board, 2003. Oil in the Sea III. Inputs, Fates, and Effects. National Academies Press, Washington, D.C.
O'Connor, B.S., Muller-Karger, F.E., Nero, R.W., Hu, C., Peebles, E.B., 2016. The role of Mississippi River discharge in offshore phytoplankton blooming in the North-eastern Gulf of Mexico during August 2010. Remote Sens. Environ. 173, 133–144. http://dx.doi.org/10.1016/j.rse.2015.11.004.
Pandey, P.C., Kumar, P., Tomar, V., Rani, M., Katiyar, S., Nathawat, M.S., 2015. Modelling spatial variation of fluoride pollutant using geospatial approach in the surrounding environment of an aluminium industries. Environ. Earth Sci. 74, 7801–7812. http://dx.doi.org/10.1007/s12665-015-4563-8.
Parinos, C., Gogou, a, Bouloubassi, I., Pedrosa-Pàmies, R., Hatzianestis, I., Sanchez-Vidal, a., Rousakis, G., Velaoras, D., Krokos, G., Lykousis, V., 2013. Occurrence, sources and transport pathways of natural and anthropogenic hydrocarbons in deep-sea sediments of the eastern Mediterranean Sea. Biogeosciences 10, 6069–6089. http://dx.doi.org/10.5194/bg-10-6069-2013.
Passow, U., Ziervogel, K., Asper, V., Diercks, A., 2012. Marine snow formation in the aftermath of the Deepwater Horizon oil spill in the Gulf of Mexico. Environ. Res. Lett. 7, 35301. http://dx.doi.org/10.1088/1748-9326/7/3/035301.
Radović, J.R., Aeppli, C., Nelson, R.K., Jimenez, N., Reddy, C.M., Bayona, J.M., Albaigés, J., 2014. Assessment of photochemical processes in marine oil spill fingerprinting. Mar. Pollut. Bull. 79, 268–277. http://dx.doi.org/10.1016/j.marpolbul.2013.11.029.
Reddy, C.M., Eglinton, T.I., Hounshell, A., White, H.K., Xu, L., Gaines, R.B., Frysinger, G.S., Reddy Eglinton, T.I., Hounshell, A., White, H.K., Xu, L., Gaines, R.B., Frysinger, G.S., 2002. The West Falmouth oil spill: the persistence of petroleum hydrocarbons in marsh sediments, 36,,. C.M., 2002 Environ. Sci. Technol. 36, 4754–4760.
Reddy, C.M., Arey, J.S., Seewald, J.S., Sylva, S.P., Lemkau, K.L., Nelson, R.K., Carmichael, C.A., McIntyre, C.P., Fenwick, J., Ventura, G.T., Van Mooy, B. a. S., Camilli, R., 2011a. Science applications in the Deepwater Horizon oil spill special feature: composition and fate of gas and oil released to the water column during the Deepwater Horizon oil spill. Proc. Natl. Acad. Sci. U. S. A. 1–9. http://dx.doi.org/10.1073/pnas.1101242108.
Reddy, C.M., Arey, J.S., Seewald, J.S., Sylva, S.P., Lemkau, K.L., Nelson, R.K., Carmichael, C., McIntyre, C.P., Fenwick, J., Ventura, G.T., Van Mooy, B.a S., Camilli, R., 2011b. Composition and fate of gas and oil released to the water column during the Deepwater Horizon oil spill. Proc. Natl. Acad. Sci. U. S. A. 109, 20229–20234. http://dx.doi.org/10.1073/pnas.1101242108.
Romero, I.C., Schwing, P.T., Brooks, G.R., Larson, R. a., Hastings, D.W., Flower, B.P., Goddard, E. a., Hollander, D.J., 2015. Hydrocarbons in Deep-sea Sediments Following the 2010 Deepwater Horizon Blowout in the Northeast Gulf of Mexico 1–23. http://dx.doi.org/10.1371/journal.pone.0128371.
Ross, C.B., Gardner, W.D., Richardson, M.J., Asper, V.L., 2009. Currents and sediment transport in the Mississippi canyon and effects of hurricane georges. Cont. Shelf Res. 29, 1384–1396. http://dx.doi.org/10.1016/j.csr.2009.03.002.
Rowe, G.T., Kennicutt II, M.C., 2009. Northern Gulf of Mexico Continental Slope Habitats and Benthic Ecology Study: Final Report. US. Dept. of the Interior, Minerals Management. Service, Gulf of Mexico OCS Region, New Orleans, p. 456. LA. OCS Study MMS 2009-039.
Ryerson, T.B., Camilli, R., Kessler, J.D., Kujawinski, E.B., Reddy, C.M., Valentine, D.L., Atlas, E., Blake, D.R., de Gouw, J., Meinardi, S., Parrish, D.D., Peischl, J., Seewald, J.S., Warneke, C., 2012. Chemical data quantify Deepwater Horizon hydrocarbon flow rate and environmental distribution. Proc. Natl. Acad. Sci. U. S. A. 109, 20246–20253. http://dx.doi.org/10.1073/pnas.1110564109.
Schwing, P.T., Romero, I.C., Brooks, G.R., Hastings, D.W., Larson, R.A., Hollander, D.J., 2015. A decline in benthic Foraminifera following the Deepwater Horizon event in the Northeastern Gulf of Mexico. PLoS One 10, 1–22. http://dx.doi.org/10.7266/N79021PB.Funding.

Shigenaka, G., Overton, E., Meyer, B., Gao, H., Miles, S., 2015. Physical and chemical characteristics of in-situ burn residue and other environmental oil samples collected during the Deepwater Horizon spill response. In: Interspill Conference, pp. 1–2.

Snyder, R. a, Ederington-hagy, M., Hileman, F., Moss, J. a, Amick, L., Carruth, R., Head, M., Marks, J., Tominack, S., Jeffrey, W.H., 2014. Polycyclic aromatic hydrocarbon concentrations across the Florida Panhandle continental shelf and slope after the BP MC 252 well failure. Mar. Pollut. Bull. 89, 201–208. http://dx.doi.org/10.1016/j.marpolbul.2014.09.057.

Stout, S.A., Payne, J.R., 2016a. Chemical composition of floating and sunken in-situ burn residues from the Deepwater Horizon oil spill. Mar. Pollut. Bull. 108, 186–202. http://dx.doi.org/10.1016/j.marpolbul.2016.04.031.

Stout, S.A., Payne, J.R., 2016b. Macondo oil in deep-sea sediments: Part 1 – sub-sea weathering of oil deposited on the seafloor. Mar. Pollut. Bull. http://dx.doi.org/10.1016/j.marpolbul.2016.07.036.

Stout, S.A., Payne, J.R., Emsbo-Mattingly, S.D., Baker, G., 2015. Weathering of field-collected floating and stranded Macondo oils during and shortly after the Deepwater Horizon oil spill. Mar. Pollut. Bull. 105, 7–22. http://dx.doi.org/10.1016/j.marpolbul.2016.02.044.

Stout, S.A., Payne, J.R., Ricker, R.W., Baker, G., Lewis, C., 2016a. Macondo oil in deep-sea sediments: Part 2 — distribution and distinction from background and natural oil seeps. Mar. Pollut. Bull. http://dx.doi.org/10.1016/j.marpolbul.2016.07.041.

Stout, S.A., Rouhani, S., Liu, B., Oehrig, J., Ricker, R.W., Baker, G., Lewis, C., 2016b. Assessing the footprint and volume of oil deposited in deep-sea sediments following the Deepwater Horizon oil spill. Mar. Pollut. Bull. http://dx.doi.org/10.1016/j.marpolbul.2016.09.046.

Tansel, B., Fuentes, C., Sanchez, M., Predoi, K., Acevedo, M., 2011. Persistence profile of polyaromatic hydrocarbons in shallow and deep Gulf waters and sediments: effect of water temperature and sediment-water partitioning characteristics. Mar. Pollut. Bull. 62, 2659–2665. http://dx.doi.org/10.1016/j.marpolbul.2011.09.026.

Tarnecki, J.H., Patterson, W.F., 2015. Changes in red snapper diet and Trophic ecology following the Deepwater Horizon oil spill. Mar. Coast. Fish. 7, 135–147. http://dx.doi.org/10.1080/19425120.2015.1020402.

Turner, R.E., Overton, E.B., Meyer, B.M., Miles, M.S., McClenachan, G., Hooper-Bui, L., Engel, A.S., Swenson, E.M., Lee, J.M., Milan, C.S., Gao, H., 2014. Distribution and recovery trajectory of Macondo (Mississippi Canyon 252) oil in Louisiana coastal wetlands. Mar. Pollut. Bull. 87, 57–67. http://dx.doi.org/10.1016/j.marpolbul.2014.08.011.

U.S. District Court, 2015. Findings of Facts and Conclusions of Law - Phase 2 Trial. Case 2: 10-md-02179-cjb-ss, pp. 1–44. Document 14021 Filed Jan. 15, 2015. http://www.laed.uscourts.gov/sites/default/files/OilSpill/Orders/1152015FindingsPhaseTwo.pdf.

Valentine, D.L., Fisher, G.B., Bagby, S.C., Nelson, R.K., Reddy, C.M., Sylva, S.P., Woo, M. a., 2014. Fallout plume of submerged oil from Deepwater Horizon. Proc. Natl. Acad. Sci. http://dx.doi.org/10.1073/pnas.1414873111.

Wade, T.L., Sericano, J.L., Sweet, S.T., Knap, A.H., Guinasso, N.L., 2016. Spatial and temporal distribution of water column total polycyclic aromatic hydrocarbons (PAH) and total petroleum hydrocarbons (TPH) from the Deepwater Horizon (Macondo) incident. Mar. Pollut. Bull. 103, 286–293. http://dx.doi.org/10.1016/j.marpolbul.2015.12.002.

Wang, Z., Fingas, M.F., 2003. Development of oil hydrocarbon fingerprinting and identification techniques. Mar. Pollut. Bull. 47, 423–452. http://dx.doi.org/10.1016/S0025-326X(03)00215-7.

Wang, Z., Stout, S. a., Fingas, M., 2006. Forensic fingerprinting of biomarkers for oil spill characterization and source identification. Environ. Forensics 7, 105–146. http://dx.doi.org/10.1080/15275920600667104.

Wardlaw, G.D., Nelson, R.K., Reddy, C.M., Valentine, D.L., 2011. Biodegradation preference for isomers of alkylated naphthalenes and benzothiophenes in marine sediment contaminated with crude oil. Org. Geochem 42, 630–639. http://dx.doi.org/10.1016/j.orggeochem.2011.03.029.

White, H.K., Hsing, P.-Y., Cho, W., Shank, T.M., Cordes, E.E., Quattrini, A.M., Nelson, R.K., Camilli, R., Demopoulos, A.W.J., German, C.R., Brooks, J.M., Roberts, H.H., Shedd, W., Reddy, C.M., Fisher, C.R., 2012. Impact of the Deepwater Horizon oil spill on a deep-water coral community in the Gulf of Mexico. PNAs. http://dx.doi.org/10.1073/pnas.1118029109.

Yan, B., Passow, U., Chanton, J.P., Nöthig, E.-M., Asper, V., Sweet, J., Pitiranggon, M., Diercks, A., Pak, D., 2016. Sustained deposition of contaminants from the Deepwater Horizon spill. Proc. Natl. Acad. Sci. 113 http://dx.doi.org/10.1073/pnas.1513156113.

Yunker, M.B., Macdonald, R.W., 2003. Alkane and PAH depositional history, sources and fluxes in sediments from the Fraser River Basin and Strait of Georgia, Canada. Org. Geochem 34, 1429–1454. http://dx.doi.org/10.1016/S0146-6380(03)00136-0.

Ziervogel, K., Dike, C., Asper, V., Montoya, J., Battles, J., D'souza, N., Passow, U., Diercks, a., Esch, M., Joye, S., Dewald, C., Arnosti, C., 2015. Enhanced particle fluxes and heterotrophic bacterial activities in Gulf of Mexico bottom waters following storm-induced sediment resuspension. Deep Sea Res. Part II Top. Stud. Oceanogr. http://dx.doi.org/10.1016/j.dsr2.2015.06.017.